The Synchronic Frame of Photospheric Magnetic Flux: The Improved Synoptic Frame

X. P. Zhao, J. T. Hoeksema and P. H. Scherrer
W. W. Hansen Experimental Physics Laboratory, Stanford University

Short title: SYNCHRONIC FRAMES

Abstract.

An iteration algorithm is developed to accurately invert Carrington longitudes to corresponding central meridian passing times and to estimate the effect of differential rotation of magnetic features on the surface field distribution. It is shown that the magnetic elements from a synoptic chart do not cover the whole solar surface at any time within the period of one solar rotation. By removing the effect of the differention rotation in synoptic charts, the "synchronic chart" can be constructed where the Carrington longitude distribution has been replaced by the heliographic longitude distribution. By combining the remapped magnetogram at a target time with the synchronic chart at the same time, the mapping inconsistence in the synoptic frame can be corrected to become the "synchronic frame" where the absccisa is expressed fully by the heliographic longitude. It has been shown that the effect of the differential rotation on the distribution of photospheric field strength and polarity is significant, and the coronal holes and the base of the heliospheric current sheet reproduced using the synchronic frame appear to be slightly better than that reproduced using the synoptic frame, showing that the synchronic frmae is a better proxy of the instantaneous whole surface distribution of photospheric magnetic field than the synoptic frame. It is suggested that as an initial, instantaneous whole-surface distribution of the photospheric magnetic field, the synchronic frame may be inputed into photospheric flux transpot models to predict better instantaneous photospheric field distribution on the portions of solar surface that are poor or not observed.

1. Introduction

Synoptic charts of the photospheric magnetic field [Bumba and Howard, 1965] have been assumed to be a proxy of the whole solar surface distribution of the photospheric magnetic field in one solar rotation period, and used as an inner boundary condition of various global coronal models. Such large-scale, long-lived, stable coronal structures as coronal streamers, coronal holes and the streamer belt have been successfully replicated on the basis of the magnetic synoptic charts. Magnetic synoptic charts are made from consecutive remapped magnetogram observed over one Carrington rotation period. Each remapped magnetogram (see the top panel of Figure 1) is sliced a strip centered at the central meridian, and all obtained strips are ranged from right to left in the order of time or from left to right in the order of the Carrington longitude (see top and bottom labels of the middle panel). Because of the differential rotation of magnetic elements, the solar surface distribution of the photospheric magnetic field is time-dependent even for the large-scale quiet field that is supposed to be constant in time. It implies that magnetic synoptic charts can be assumed to be whole surface distribution of photospheric magnetic field only when the modeled structures, such as the location and shape of cornal streamers and coronal holes, are pretty stable and rotate rigidly.

In order to track the change of transient large-scale coronal structures (say soft X-ray arcades) on the time scale much less than one solar rotation period, the "synoptic frame" has been developed as a proxy of the instantaneous whole surface distribution of the photospheric magnetic field [Zhao, Hoeksema and Scherrer, 1997]. Here the time of interest (the target time hereafter) is the observational time of interesting coronal structures. The temporal variation of the 1996 August boot-shaped coronal hole boundary on the time scale of a day and the temporal variation of the 1994 April Soft X ray arcade on the time scale less than a day have been reproduced using synoptic frames at the target times and various coronal magnetic field models [Zhao, Hoeksema and Scherrer, 1999; 2000]. As shown in Figure 1, the synoptic frame for a target time is

consist of a remapped magnetogram observed at the target time and a non-traditional synoptic chart centerted at a Carrington logitude corresponding to the target time. We replace the term of "chart" or "map" (http://gong.nso.edu/data/magmap/) with the term of "frame" to emphsize the major role played by the remapped magnetogram in the instantaneous whole surface distribution of the magnetic field. Figure 1 shows how the 1998:05:23_16:03:30 synoptic frame (the bottom panel) is constructed by replacing the central part of the non-traditional synoptic chart (the middle panel with the abscissa expressed in Carrington longitudes shown by blue vertical lines) with the 1998:05:23_16:03:30 remapped magnetogram (the top panel with the abscissa expressed in heliographic longitudes shown by black vertical lines). The abscissa of the synoptic frame here is expressed in hybrid longitude, i.e., using heliographic longitudes for the magnetogram component and using Carrington longitudes for the synoptic-chart component. This work tries to improve the mapping inconsistence in the synoptic frame so that the abscissa of synoptic frames are expressed fully by heliographic longitudes.

Ulrich and Boyden [2006] have developed a method for estimating the effect of differential rotation of magnetic features. They first add the effect of differential rotation to remapped magnetograms to transform heliographic longitude distribution to the Carrinton longitude distribution so that to reduce the smearing effect occurred in constructing synoptic charts when averaging over multiple observed strips, and then remove the effect of differential rotation in synoptic charts to obtain the whole surface distribution of fields with heliographic longitude spacing at the target time. This kind of improved synoptic charts and whole surface distribution of fields are specifically referred to, respectively, as the "Differential Rotation Corrected" (DRC) synoptic chart and the "snapshot heliographic map" in their paper.

In Section 2, we develop a different method that takes consideration the Earth's non-uniform travel around the Sun, and accurately convert Carrington longitudes to corresponding central meridian passing (CMP) times. In this way, an improved

synoptic chart with its abscissa expressed by heliographic longitude can be obtained, and termed as "synchronic chart" in what follows, which is the same as the "snapshot heliographic map" in Ulrich and Boyden [2006]. The improved synoptic frame (the "synchronic frame" in what follows) can then be easily obtained by combining the remapped magnetogram with the synchronic chart at the target time. To see the effect of the differential rotation we compare the synchronic frame with the synoptic frame in Section 3 by examing the change of field strength and polarity structures. In Section 4, we compute open field regions and the source-surface neutral line using the synchronic and synoptic frames and compare the results with observations. The summary and discussion are in the last section.

2. Construction of the synchronic chart and the synchronic frame

As mentioned above, there is the mapping inconsistence in synoptic frames. To remove the inconsistence we need to convert the Carrington longitude to the corresponding heliographic longitude for all elements in the non-traditional magnetic synoptic chart at a target time.

For the differentially rotating Sun, in order to display the location of magnetic elements on solar surface, it is necessary to first set a reference time and a referrence longitude. We set here the target time as the reference time and the value of the corresponding Carrington longitude as the value of the reference heliographic longitude of the corresponding meridian. For instance, the time of 1998:05:23_16:03:30 and the heliographic longitude of 1998.05.23:200° in Figure 1 (Note, the Carrington longitude is expressed as 1936:200°). For magnetic elements located along a Carrington longitude corresponding to the other CMP time, the heliographic longitudes the magnetic elements used to or will be located at the reference time may be calculated on the basis of the

latitudes the elements located and the time difference from the reference time.

2.1. Inversion of Carrington longitude to CMP time

The synodic rotation period varies a little during the year because of the eccentricity of the Earth's orbit. The synodic period is shortest in July and longest in January.

The Carrington longitude corresponding to a CMP time can be accurately calculated using the formulae in The Astronominal Almanac and the CMP time. But there is no simply way to accurately invert the CMP time from a given Carrington longitude. We have developed an iteration method to accurately invert the CMP time. Firstly, we grossly estimate the CMP time from a given Carrington longitude on the basis of a specifying Carrington longitude corresponding to a specific CMP time (Say CR1891:349.04 that corresponds to the CMP time of 1995:01:01_00h:00m:00s) and the constant synodic rotation period of 27.2753 days. We then calculate the Carrington longitude from such a estimated CMP time. By iteratively adjust the estimated CMP time, the calculated Carrington longitude finally approaches the given Carrington ngton longitude so that the CMP time corresponding to the given Carrington longitude can be accurately determined.

To show the annual variation of the difference of such obtained CMP times, we invert the difference of CMP times corresponding to the difference of two pairs of Carrington longitudes, (180°, 160°) and (180°, 5°), over 15 solar rotations from Carrington number 2075 to 2089 (or from 2008:10:10 to 2009:11:03). The red curves in Figure 2 are obtained using the iteration method. The annual variation of the red curves is consistent with the annual variation of the synodic rotation period. The blue lines in Figure 2 are obtained using Ulrich and Boyden [2006] method, i.e., multiplying the difference of Carrington times by 360° and then devided the result by the Carrington rotation rate. The blue lines would be similar to the red curves if devided the result by varying synoptic rotation rates. Figure 2 shows that the effect of varying synodic

rotation rate may not be neglected when the separation of two Carrington longitudes greater than 20°.

2.2. The effect of the differential rotation on the location of magnetic elements

The sidereal or synodic rotation rate of photospheric magnetic features is latitude-dependent and expressed as Equation (1) where θ denotes the heliographic latitude of magnetic elements; the coefficients A, B and C vary depending on the selected magnetic feature and analytic method.

$$\omega(\theta) = A + B\sin^2(\theta) + C\sin^4(\theta) \tag{1}$$

A few sets of coefficients have been tested, and it is found that only the widely-used Snodgrass (1983) rotation rate can be used to find the heliographic latitude of $\pm 16.46°$, as expected. The coefficients for the synodic differential rotation rate are $A = 13.3445$, $B = -1.56154$, and and $C = -2.23407$ in $\circ/day$.

The middle panels in Figure 3 show the effect of the differential rotation on the location of magnetic elements. The red vertical line in the middle panel denote both the Carrington longitude of CR1936:200° and the reference longitude, i.e., the heliographic longitude of 1998.05.23:200° which corresponds to the reference time of 1998.05.23_16:03:30. The blue vertical lines denote the Carrington longitudes corresponding to other times. The difference of the blue vertical lines from the red one denotes the time difference. Each black or red curve show the locus of heliographic longitudes calculated using the time difference. The two horizontal dotted lines denote locus of latitudes where the differential rotation rate equals the Carrington rotation rate. As shown in the panel, all blue vertical lines that are associated with all black curves are located within the 1998.05.23:200° non-traditional synoptic chart, and there are four blank corners where no black curves exist, demonstrating that the magnetic

elements in the 1998.05.23:200° non-traditional synoptic chart (in fact, any synoptic chart) cannot be used to completely fill in the whole solar surface at any instant within the period of the rotation. To construct a magnetic synchronic chart more observational data than that one solar rotation are needed. As shown by the red curves, the left (right) quadrant of the non-traditional synoptic chart that occurs before (after) the CR1936:200° synoptic chart are needed for filling up the right (left) blank corners (see the top panel) (see the top panel).

2.3. Construction of magnetic synchronic charts and synchronic frames

The magnetic field distribution will change because of the shifts of heliographic longitudes relative to corresponding Carrington longitudes. As shown by the middle panel of Figure 3, the change of the magnetic field distribution will be significant at latitudes higher than 30°, i.e., the locations of older, decaying active regions, unipolar magnetic regions, and polar regions. Except for the effect of differential rotation, these large-scale photospheric fields may be nearly time-independent over one solar rotation. Thus the time variation of these large-scale photospheric fields caused by the differential rotation can be effectively corrected as follows.

To obtain the magnetic field distribution in heliographic coordinates, we move magnetic elements at each blue vertical line to corresponding red or black curves and then get averages of the moved magnetic elements at the same latitude around each heliographic longitude.

The bottom panel of Figure 3 shows the MDI magnetic synchronic chart. It centers at the heliographic longitude of 1998.05.23:200°, as shown by the vertical red line and obtained using the extended non-traditional synoptic charts (top panel). It can be considered as the instantaneous magnetic field distribution over the whole solar surface at the time of 1998.05.23_16.03.30 if the evolution of the photospheric magnetic field in the period of time is caused purely by the differential rotation.

The synchronic frame is thus obtained by merging the remapped magnetogram (the top panel of Figure 1) with the synchronic chart (the bottom panel of Figure 3).

3. The effect of differential rotation on the distribution of the field strength and polarity structures

To see if the technique developed here works we first compare the field strength distribution between the synchronic and synoptic charts.

Figure 4 displays the longitudinal variation of magnetic field strength at latitudes of $-84°$, $-60°$, $-30°$, $-16circ$, and $0°$. Blue (red) lines denote the longitudinal variation in the synchronic (synoptic) frames. As expected, there is no shift between the blue and red lines at latitude of $16°$, where the differential rotation rate is the same as the Carrington rotation rate. Above (below) the latitude of $16°$ the blue line significantly shifts, relative to the red line, toward (away from) the black vertical line from two sides. The shift increases as the heliographic longitude aways from the black line and as the latitude increases. The effect of the differential rotation on magnetic polarity distribution should also be detectable. Figure 5 shows a quantitative sketch of the effect. The rectangles bound by thick (thin) line denote the areas occupied by magnetic structures in the synchronic (non-traditional synoptic) chart. Depending on the latitude and the longitudinal distance from the center, the thick line rectangles, relative to the thin line rectangles, displace toward the center with their upper parts shear more than the lower parts and their rear parts move more than front parts.

Such differences are perceptible in the bottom panel of Figure 3. All active regions away from the red line in the panel show a displacement toward the red line with respect to the top panel. For instance, the active regions located at $\pm 30°$ of latitude and 98.05.23_$350°$ of longitude moved about $5°$ leftward relative their counterpart in the bottom panel of Figure 1. In addition, the active region in northern (southern)

hemisphere in the bottom panel of Figure 3 shows a slight counter clock-wise (clock-wise) rotation with respect to the bottom panel of Figure 1. The structures in the east side shows an opposite rotation. This tendency of rotation is consistent with Figure 4.

4. Effect of differential rotation on modeled coronal structures

To see if the Effect of differential rotation on modeled coronal structures is significant, we compute the open field regions and the source surface neutral line by inputing the synchronic and synoptic frames into the potential field-source surface model.

The top two panels of Figure 6 display the synoptic and synchronic frames. Overplotted are the photospheric polarity inversion lines of large-scale field (black curves). Between the two panels differences like those found in Figures 3 and 4 also appear in the synoptic chart portion outside the rectangle bound by dashed lines. The displacing, tilting and shrinking of the positive (white) and negative (black) regions bound by polarity inversion lines in the second panel indicate the effect of the differential rotation on the distribution of magnetic polarity structures.

What is the effect of this difference on the calculated coronal field, specifically, on modeled coronal holes and the base of the heliospheric current sheet (HCS)?

The bottom two panels of Figure 6 display positive and negative (blue and red) open field regions, the source surface field strength distribution (see contours in grey images) and the neutral lines (black curves). The source surface is located at 2.5 solar radii and the principal order of the spherical harmonic series being 45. The green line in the bottom panel is the same as the neutral line in the third panel, showing the difference between the two neutral lines caused by the correction of differential rotation. The difference of calculated coronal holes between the two panels are evident in the synoptic chart portion outside the the rectangle. Even in the magnetogram portion within the rectangle both the neutral line and the northern and near-equator open field

regions show the perceptible difference.

Figure 6 shows that although the correction changes the photospheric field distribution only in the portion outside the rectangle, calculated coronal holes and the HCS are changed in the portion within the rectangle as well as in the portion outside the rectangle. To see whether or not the magnetic synchronic frame better represents the instantaneous whole surface distribution of the photospheric magnetic field than the synoptic frame, it is necessary to compare the modeled coronal and heliospheric structures overlying the rectangle with observations made at the same time.

5. Comparison of modeled coronal hole with observations

Since the synchronic frame is a proxy for the global distribution of the photospheric field at a specific time, the coronal structure and the HCS to be compared must be observed near the same time. The outlines in Figure 6 show the boundary of 1083 nm coronal holes observed at 1998.05.23_17:13 by the NSO Vacuum Telescope of the Kitt Peak Observatory. Although for south polar hole and the near-equator hole, the agreement between observation and both calculations is basically the same, the blue foot point areas in the north polar hole calculated using synchronic frame does show a better agreement with observations than the synoptic frame.

6. Summary and Discussion

We have shown that the magnetic elements from a magnetic synoptic chart cannot be used to fill up the whole solar surface at any time within the period of a rotation.

We conclude that the effect of differential rotation on the surface distribution of photospheric magnetic field should be taken into consideration in constructing the instantaneous whole-surface distribution of magnetic fields, the magnetic synchronic frame, and that the technique developed here is efficient in correcting the effect of the differential rotation for synoptic charts.

The difference between the synchronic and synoptic frames is detactable but not dramatic, as expected. That is why the synoptic frame, as the first approximation, can be used, to track the change in coronal hole boundary and X-ray arcade on the time scale of a day.

The coronal holes calculated using the synchronic frame appear to agree with the observation slightly better than that using the synoptic frame.

It may be only the magnetic synchronic frames that may be used to reproduce the different coronal and heliospheric structures that are located, respectively, under different spacecraft (such as the SOHO and the STEREO A and B) and observed at the same time.

The evolution of the photospheric magnetic field depends on other ingredients as well as the differential rotation. Flux transport models that incorporates flux emergence, random-walk dispersal, meridional advection, differential rotation, and removal of flux via cancellation (Schrijver and Derosa, 2003, and references therein), can be used to simulate the evolution of the photospheric magnetic flux from instant to instant over the whole solar surface. The Flux transport models need an initial, instantaneous whole surface distribution of the photospheric magnetic flux as an input. The synchronic frame is an input to the models much better than the magnetic synoptic chart. What predicted from the models and the magnetic synchronic frame is expected to be closer to the realistic whole-surface distribution than what from the magnetic synoptic chart.

7. Acknowledgments

References

Bumba, B. and R. Howard, *Astrophys. J., 141*, 1502, 1965.

Pevtsov, A. A. and S. M. Latushko, *Astrophys. J., 528*, 999, 2000.

Schrijver, C. J. and DeRosa, M. L., *Solar Physics, 212*, 165, 2003.

Ulrich, R. K. and J. Boyden, *Solar Phys., 235*, 17, 2006.

Zhao, X. P., J. T. Hoeksema, P. H. Scherrer, *The Proceedings of the Fifth SOHO Workshop at Oslo*, SH-404, p. 751, 1997.

Zhao, X. P., J. T. Hoeksema, P. H. Scherrer, *J. Geophys. Res., 104*, p. 9735, 1999.

Zhao, X. P., J. T. Hoeksema, P. H. Scherrer, *Astrophys. J., 538*, 932, 2000.

X. P. Zhao, W. W. Hansen Experimental Physics Laboratory, Stanford University, Stanford, CA 94305-4085. (e-mail: xuepu@quake.stanford.edu)

J. T. Hoeksema, W. W. Hansen Experimental Physics Laboratory, Stanford University, Stanford, CA 94305-4085. (e-mail: jthoeksema@solar.stanford.edu)

P. H. Scherrer, W. W. Hansen Experimental Physics Laboratory, Stanford University, Stanford, CA 94305-4085. (e-mail: phscherrer@solar.stanford.edu)

Received _____

Second Version: Sept. 2, 2009

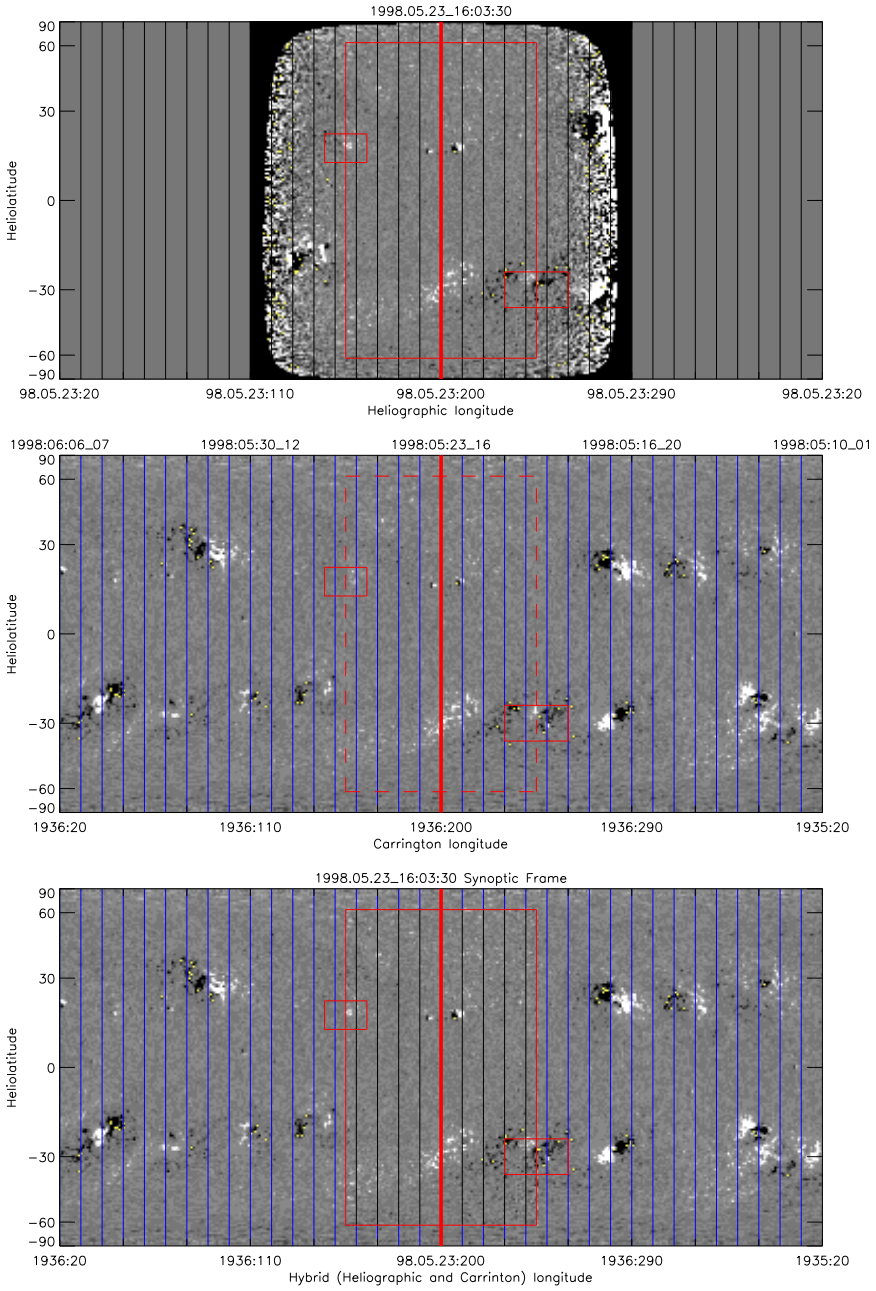

Figure 1. Construction of the synoptic frame of the photospheric magnetic field (bottom panel) using a remapped magnetogram (top panel) and an non-traditional synoptic chart (middle panel). Black and blue vertical lines denote, respectively, Heliographic and Carrington longitudes. The abscissa in bottom panel is in hibrid longitude.

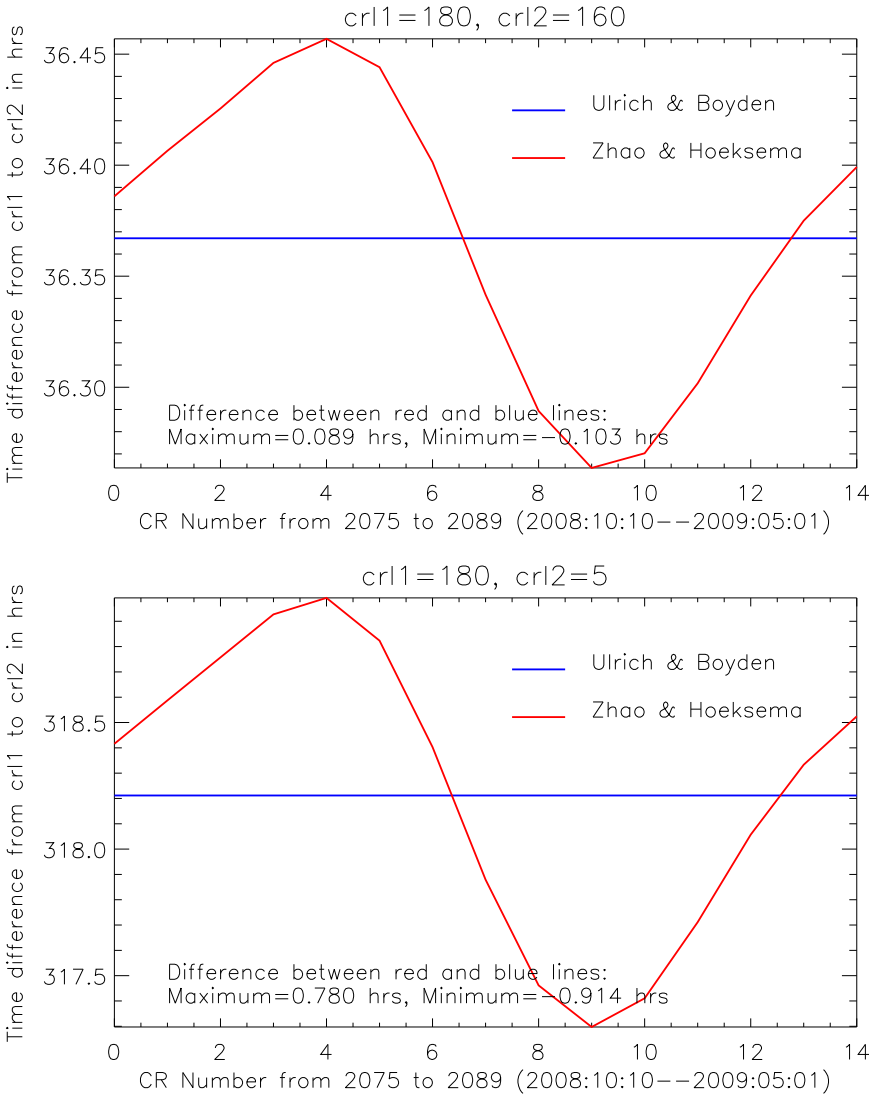

Figure 2. Comparision of time differences inverted using two methods

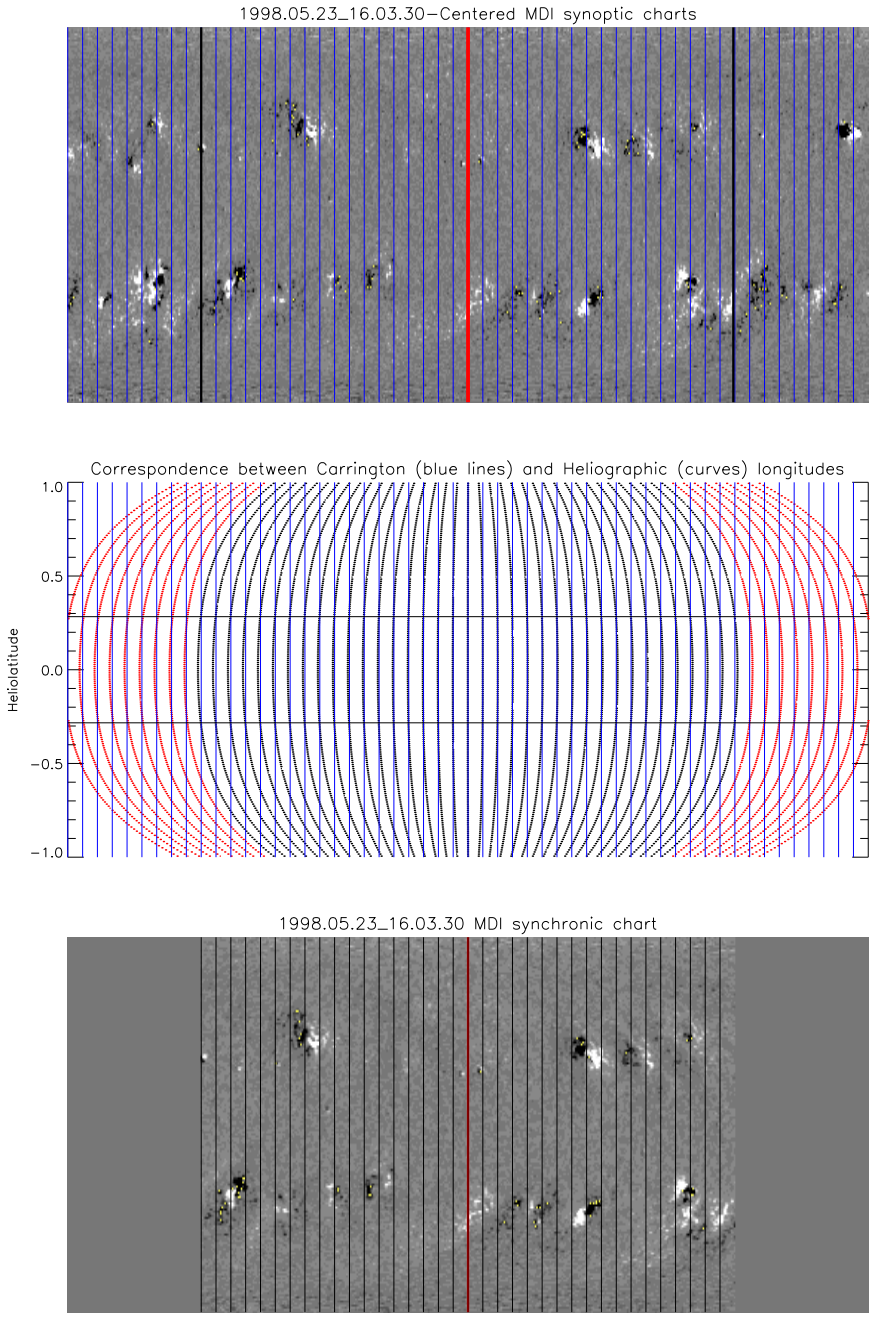

Figure 3. Construction of synchronic charts (bottom panel) from non-traditional synoptic charts (top panel). The abscissa in top (bottom) panel is in Carrington (Heliographic) longitude (see text for details).

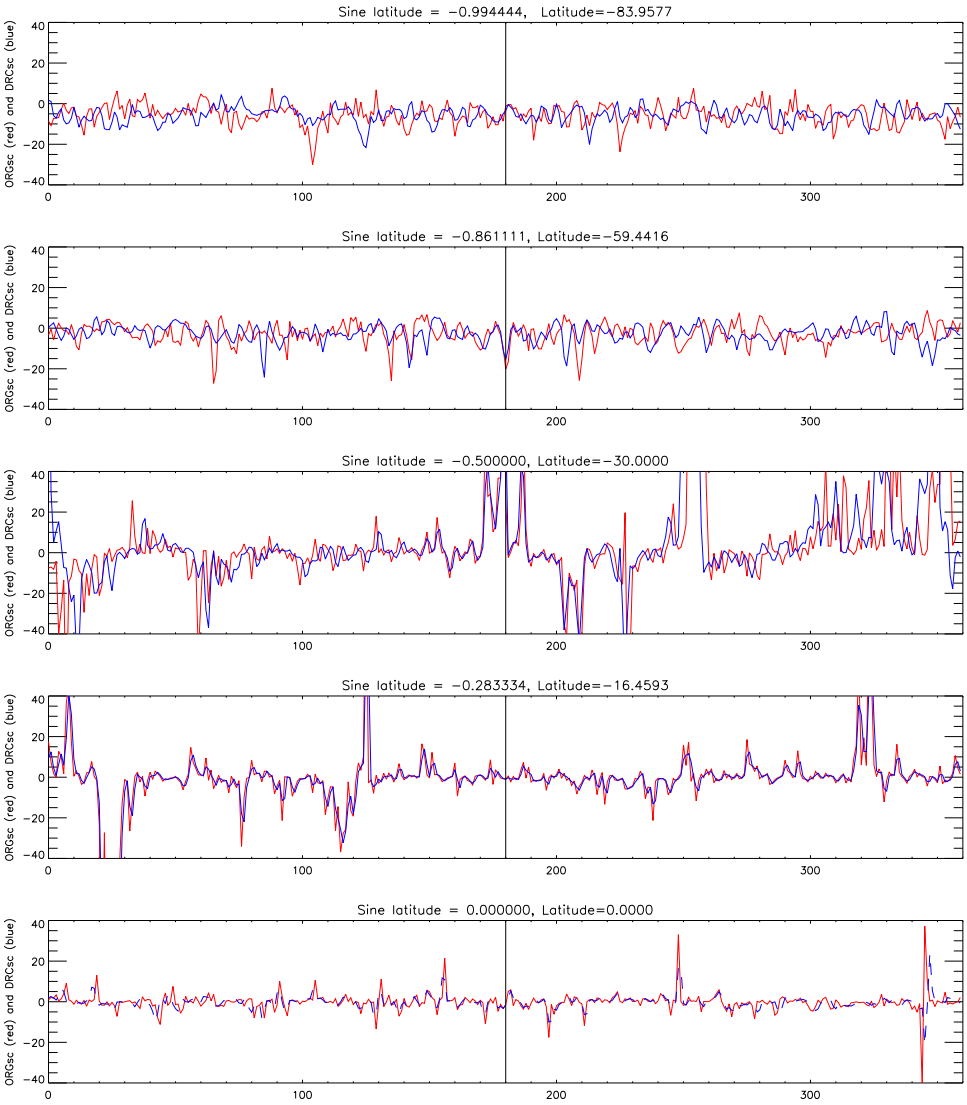

Figure 4. Comparison of the longitudinal variation of magnetic field at latitudes of 0, 16, 30, 60 and 84° (bottom to top) between non-traditional synoptic charts (red lines) and synchronic charts (blue lines).

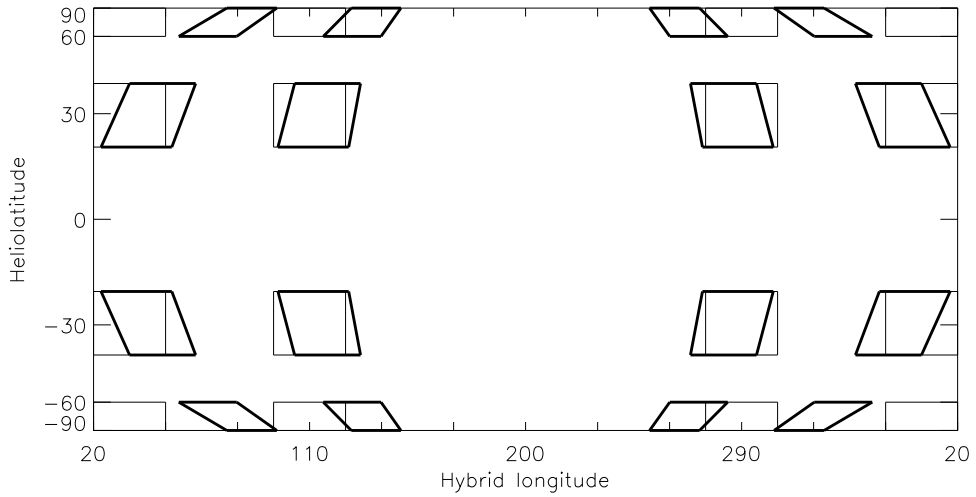

Figure 5. Comparison between non-traditional synoptic charts (thin outlines) and synchronic charts (thick outlines), showing the effect of differential rotation on magnetic structures.

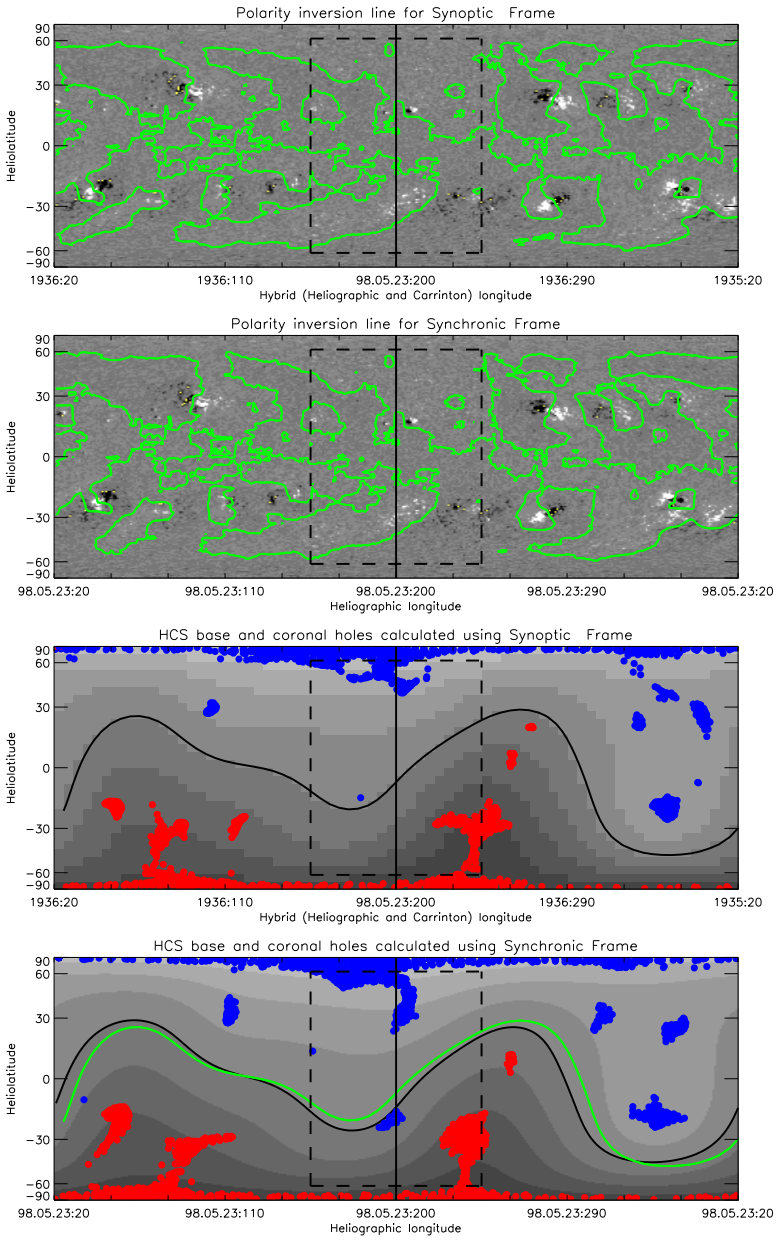

Figure 6. Comparison between synoptic frames (the first panel) and synchronic frame (the second panel). The green lines in the two panels are polarity inversion lines. The third and fourth panels shows the foot-points of open field lines (blue-positive and red-negative) and source surface neutral lines calculated using the first and second panels, respectively.

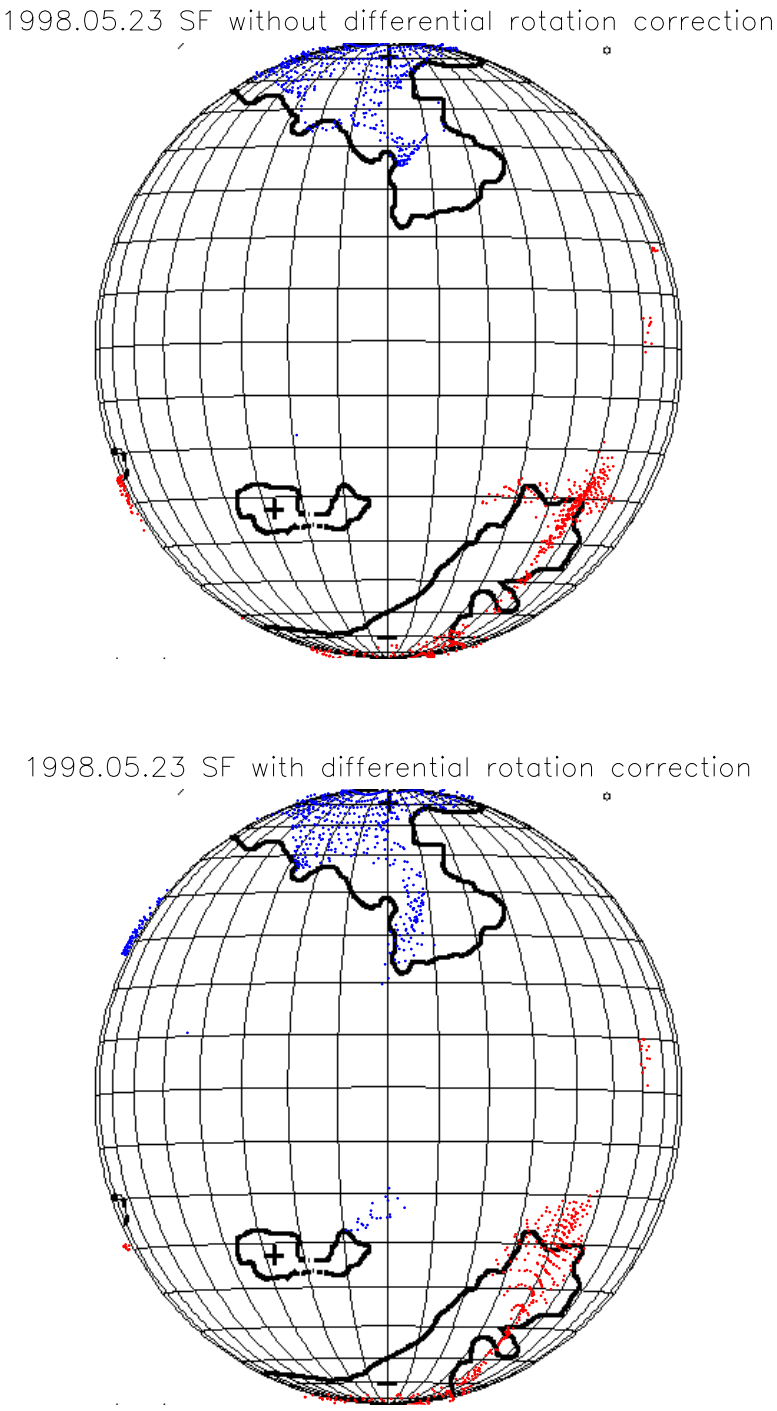

Figure 7. Comparison of open field regions calculated using the 1998.05.23_16:03:30 synoptic frame and the synchronic frame with KPNO He 1083.0 nm coronal holes observed at 1998.05.23_17.43.